Appl Phys B (2009) 96: 355–361
DOI 10.1007/s00340-009-3480-5

Applied Physics B
Lasers and Optics

Two-dimensional dissimilar electromagnetic cloak for irregular regions

K. Yao · C. Li · F. Li

Received: 10 December 2008 / Revised version: 23 February 2009 / Published online: 3 April 2009

Abstract A general method to design a 2D dissimilar cloak for irregular regions is presented by operating a nonlinear transformation in polar coordinates. The material parameters avoid discontinuities while the thickness of the cloak shell is effectively limited in elongated directions. Full-wave simulations of an elliptic cloak, a rectangular cloak, and an arbitrary-shape cloak are performed to verify the validity of the design. Both the material parameters and the scattering widths of different models are calculated and illustrated for comparison. This method provides a possible approach for designing complex shaped cloaks.

PACS 41.20.Jb · 42.25.Gy · 42.25.Fx

1 Introduction

Recently, transformation optics, especially invisibility cloaks based on coordinate transformation, has received intense attention. The basic idea of this method is the equivalence between trajectories propagating through the warped space, which can be considered as the topological interpretation, and propagating through the special electromagnetic structures with complex constitutive relations, which provides the material interpretation [1, 2]. For two-dimensional (2D) circular cloaks, the validity of the approach was first confirmed computationally in geometric optic limits [2], then in full-wave finite element simulations [3], and furthermore, at microwave frequencies [4] and optical frequencies [5] with the help of metamaterial technology, although a reduced set of cloak parameters was used in the experimental demonstrations. Researches from other viewpoints, such as theoretical and practical problems, have been reported [6–10], and the transformation method was even introduced into acoustic applications [11].

Up to one year ago, most studies on cloak design were limited to circular cylindrical cases (2D) and spherical cases (3D) due to the symmetry in geometry and the simplicity in calculation. After that, the square cloak [12], eccentric elliptic cloak [13], and homocentric elliptic cloak [14–16] were proposed one after the other. Furthermore, designs for ellipsoids, rounded cuboids, and rounded cylinders were also reported [17]. The authors also proposed the design of 2D cloaks with arbitrary geometries [18]. Meanwhile, high-order transformations have been analytically studied [19–21]. However, for all the examples mentioned above, the inner and outer boundaries of the cloak device are geometrically similar.

For the convenience of practical applications, especially when cloaking elongated objects, the outer boundary of the cloak shell is usually desired to be not similar to the inner boundary. Kwon and Werner proposed a 2D elliptic cloak design having a uniform thickness by using the spatial transformation in a composite coordinate system [22]. The cloak, which is a union of two annular regions of uniform thicknesses, involves discontinuous constitutive parameters across the interface, and is therefore not easy to calculate or fabricate. Hu et al. discussed arbitrary shape transformation media from a deformation view and got noticeable results numerically [23], but the method still has difficulties in picking up material parameters to fabricate. The concept

K. Yao · C. Li (✉) · F. Li
Institute of Electronics, Chinese Academy of Sciences, Beijing 100190, China
e-mail: cli@mail.ie.ac.cn

K. Yao
e-mail: yaokan06@mails.gucas.ac.cn

F. Li
e-mail: fli@mail.ie.ac.cn

of 'reshaper' was proposed later [24], providing a general recipe for designing transformation media.

In this paper, we present a general method to design 2D dissimilar cloaks by operating a nonlinear transformation in the polar coordinate system. To show the simplicity and efficiency of this recipe, the method is applied to the elliptic cloak and approximate rectangular cloak, where a concept of superellipse is used in the latter example. An arbitrary shaped cloak is also displayed to show the generality. The designs avoid discontinuities in constitutive parameters. Furthermore, the total electric-field distributions are simulated by using the finite element method, and the scattering widths are calculated in order to quantitatively evaluate the cloaking performance. Cloaks of ideal and lossy models are compared according to the scattering width parameter.

2 Transformation equations

Consider an arbitrary continuous spatial transformation in the form

$$x^{\alpha'}(x^{\alpha}) = \Lambda_{\alpha}^{\alpha'} x^{\alpha}. \tag{1}$$

Here $\Lambda_{\alpha}^{\alpha'} = \frac{\partial x^{\alpha'}}{\partial x^{\alpha}}$ is the Jacobian transformation matrix, while the primed indices denote vectors in the transformed space. As tensor densities of weight $+1$, the associated permittivity and permeability transform as [2, 25]

$$\begin{aligned} \varepsilon^{i'j'} &= \det\bigl(\Lambda_i^{i'}\bigr)^{-1} \Lambda_i^{i'} \Lambda_j^{j'} \varepsilon^{ij}, \\ \mu^{i'j'} &= \det\bigl(\Lambda_i^{i'}\bigr)^{-1} \Lambda_i^{i'} \Lambda_j^{j'} \mu^{ij}. \end{aligned} \tag{2}$$

The absolute value signs of the determinant are dropped, as the transformations we discuss are warping and squeezing, where the determinants are always positive.

In polar coordinates, the boundary of an object to be cloaked, i.e. the inner boundary of the cloak shell, can be expressed as

$$f_{\text{in}} = a \cdot \rho(\theta), \tag{3}$$

where $\rho(\theta)$ is the normalized polar equation obtained by setting $\rho(0) = 1$, and a can be comprehended as a radial scale factor. In the same way, suppose the outer boundary to be

$$f_{\text{out}} = b \cdot \varphi(\theta). \tag{4}$$

Since the cloaking transformations are conducted in the radial direction, to form a dissimilar cloak, we define a nonlinear function

$$r' = a + \frac{b\varphi(\theta) - a\rho(\theta)}{b\varphi(\theta)} \cdot r, \tag{5}$$

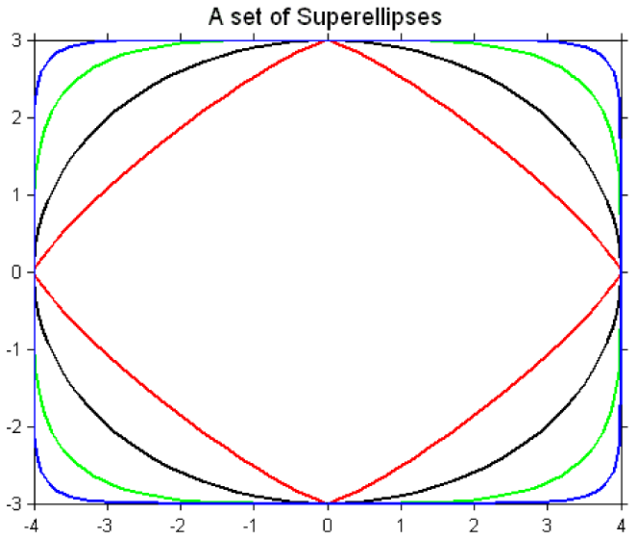

Fig. 1 A set of superellipses, in which $x_0 = 4$, $y_0 = 3$, and index n is substituted by 1.2 (*red*), 2 (*black*, *ellipse*), 4 (*green*), 10 (*blue*) in turn from inner to outer boundary

where r and r' represent the radial scale factors normalized to $\rho(\theta)$ in the original space and the transformed space, respectively. Meanwhile no operation is defined in the θ- or z-direction.

Obviously, (5) achieves results that take all the fields illuminating on the device and compress them into the region between $f_{\text{in}}(\theta)$ and $f_{\text{out}}(\theta)$, i.e. the cloak shell. In contrast to the transformations previously presented, (5) ensures different squeezing scales in different directions, which leads to unsymmetrical warping of the space (the topological interpretation) and more complex changing of the constitutive parameters (the material interpretation). For the special case that $\rho(\theta) = \varphi(\theta)$, the transformation relation degenerates to a very simple form according to (5), which reveals the symmetrical squeezing scale in a similar cloak.

2.1 Elliptic cloak

For an ellipse with its semi-axes lying along x-, y-directions of length x_0 and y_0, respectively, the polar equation can be expressed as

$$f_{\text{in}}(\theta) = \frac{x_0}{[\cos^2\theta + (x_0 \sin\theta / y_0)^2]^{1/2}}. \tag{6}$$

Considering the geometric properties of ellipses, an ellipse as described in (7) can be very close to the geometry that is defined by giving a thickness increment Δ to the ellipse in (6):

$$f_{\text{out}}(\theta) = \frac{x_0 + \Delta}{\{\cos^2\theta + [(x_0 + \Delta)\sin\theta / (y_0 + \Delta)]^2\}^{1/2}}. \tag{7}$$

A dissimilar elliptic cloak can be realized by substituting (5), (6), (7) into (2) [18]. The cloak device consists of only

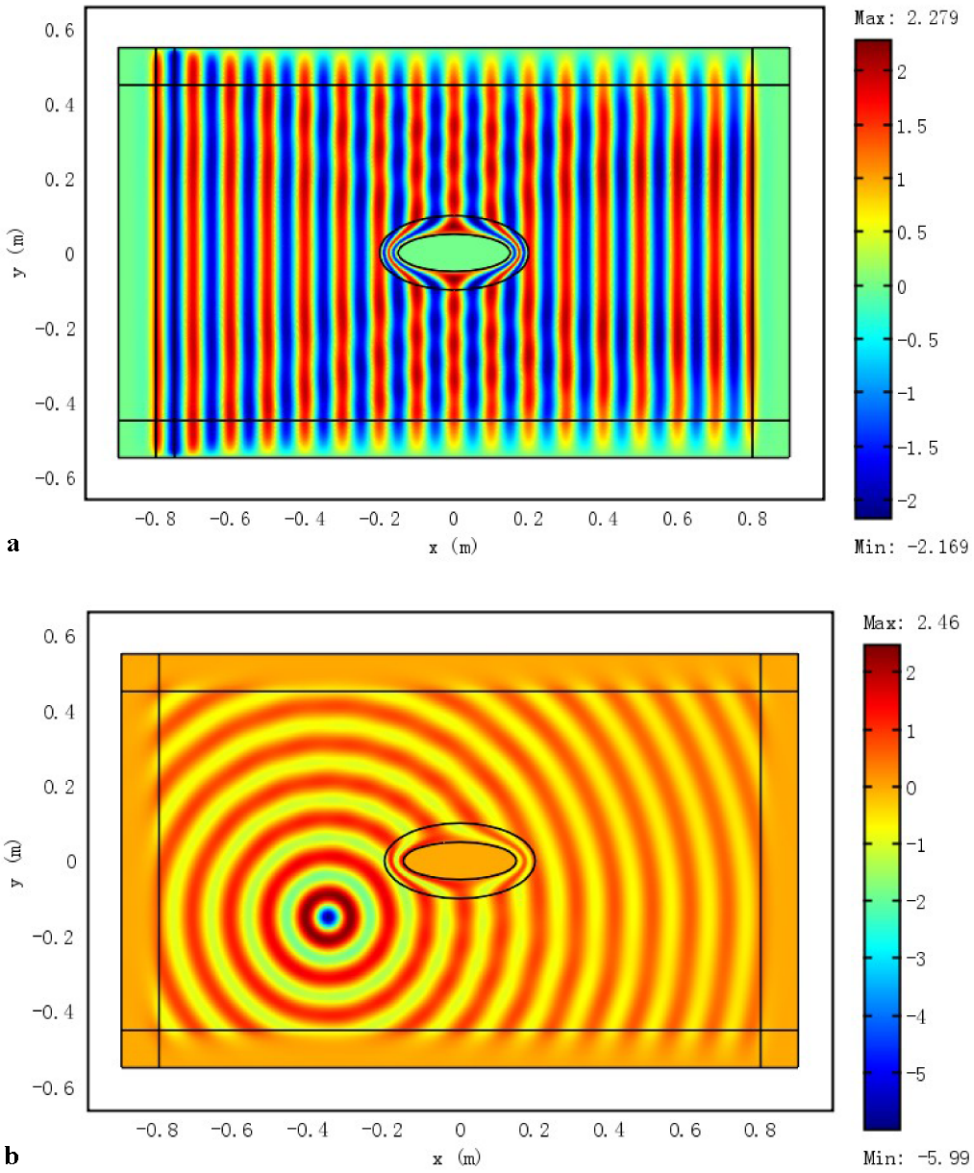

Fig. 2 Simulation results of the total electric-field distribution in the dissimilar elliptic case, in which $a_1 = 0.15$ m, $b_1 = 0.05$ m for the inner boundary, and $a_2 = 0.20$ m, $b_2 = 0.10$ m for the outer boundary. (**a**) Illuminated by a plane wave. (**b**) Illuminated by a cylindrical wave

one annular outside the inner object, and therefore does not involve discontinuity problems. The thickness of the annular is remarkably limited due to (7), especially in the direction of a major axis.

2.2 Approximate rectangular cloak

Rahm et al. have proposed a cloak device of square cross section. However, a rigorous square cloak, which possesses sharp corners, has challenges not only in the continuity of material parameters, but also in thickness when generalized to rectangles because of the similar geometry of the boundaries. We apply the superellipse as the approximation of the rectangle. The approach does not contain discontinuities in parameters, and is convenient combined with dissimilar cloaks to overcome the thickness problem.

As a generalization of the ellipse, the polar equation of a superellipse is

$$f_{\text{in}}(\theta) = \frac{x_0}{(|\cos\theta|^n + |x_0 \sin\theta / y_0|^n)^{1/n}}. \tag{8}$$

The curve described by (8) approaches a rectangle quickly when n increases to infinity. In fact, a smaller n, taking 10 or 20 for example, can give a fairly good approximation. Moreover, the curve closes to a diamond when n approaches 1, as shown in Fig. 1.

Following the idea of (7), we can also redefine

$$f_{\text{out}}(\theta) = \frac{x_0 + \Delta}{[|\cos\theta|^n + |(x_0 + \Delta)\sin\theta / (y_0 + \Delta)|^n]^{1/n}}. \tag{9}$$

Note that, unlike the elliptic cases, the superelliptic annular between $f_{\text{in}}(\theta)$ and $f_{\text{out}}(\theta)$ approaches uniform thick-

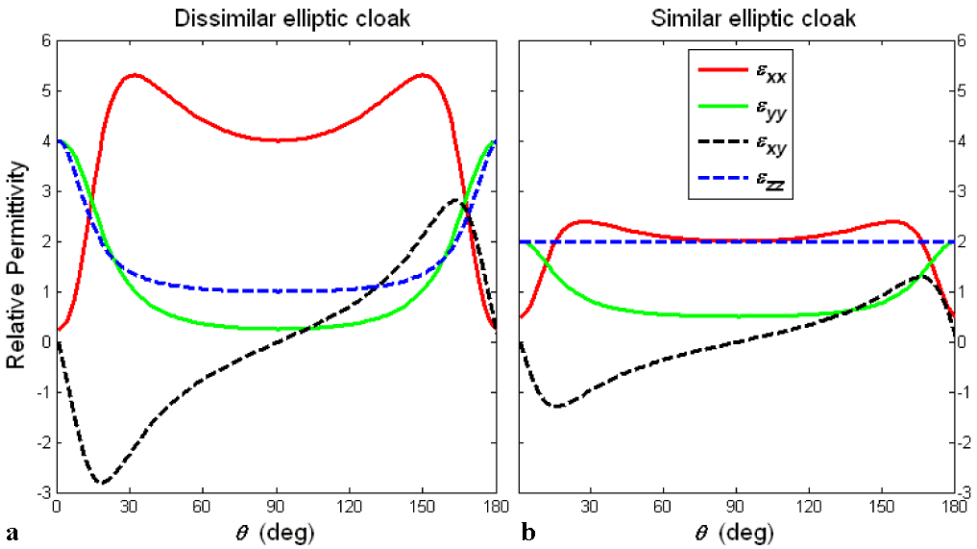

Fig. 3 Material parameters on the outer boundary for elliptic cases; only 0–180° are shown for symmetry. (**a**) Values for dissimilar ellipses, where $a_1 = 0.15$ m, $b_1 = 0.05$ m for the inner boundary, and $a_2 = 0.20$ m, $b_2 = 0.10$ m for the outer one. (**b**) Values for similar ellipses, where $a_1 = 0.15$ m, $b_1 = 0.05$ m for the inner ellipse, and $a_2 = 0.30$ m, $b_2 = 0.10$ m for the outer ellipse

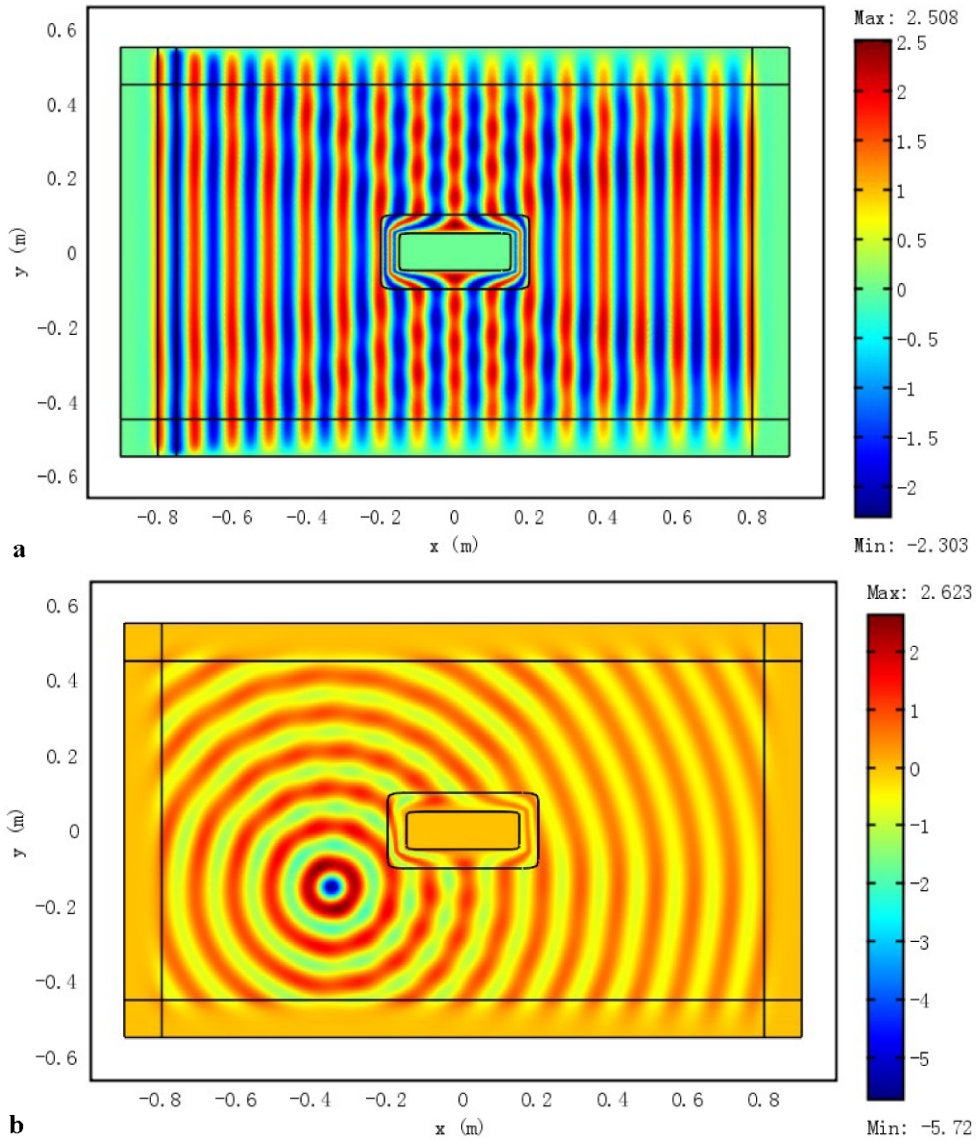

Fig. 4 Simulation results of total electric-field distribution in dissimilar approximate rectangular case, where $a_1 = 0.15$ m, $b_1 = 0.05$ m for the inner object, and $a_2 = 0.20$ m, $b_2 = 0.10$ m for the outer boundary. (**a**) Illuminated by a plane wave. (**b**) Illuminated by a cylindrical wave

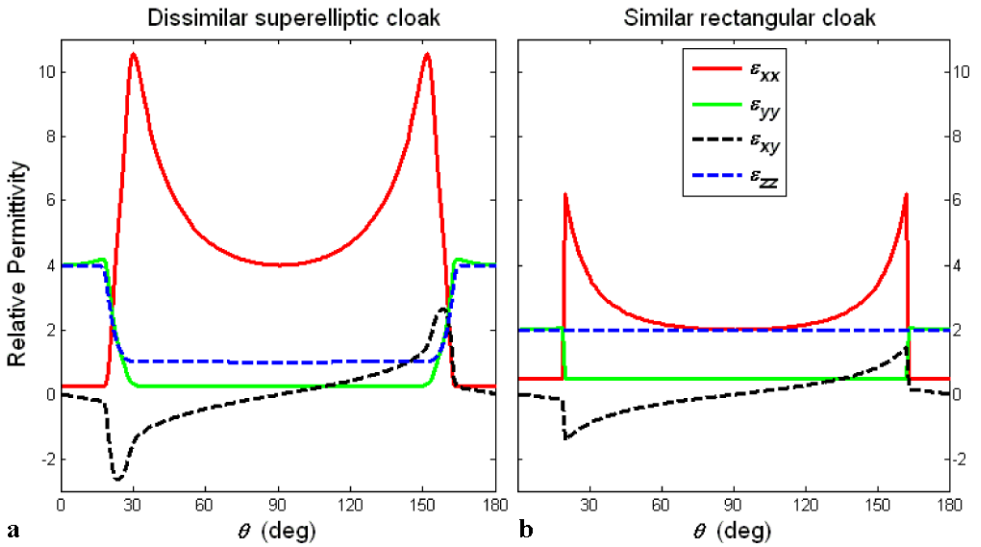

Fig. 5 Material parameters on the outer boundary for rectangular cases; only 0–180° are shown for symmetry. (**a**) Values for dissimilar approximate rectangles, in which $a_1 = 0.15$ m, $b_1 = 0.05$ m for the inner object, and $a_2 = 0.20$ m, $b_2 = 0.10$ m for outer boundary. (**b**) Values for similar rigorous rectangles, where $a_1 = 0.15$ m, $b_1 = 0.05$ m for the inner object, and $a_2 = 0.30$ m, $b_2 = 0.10$ m for the outer boundary

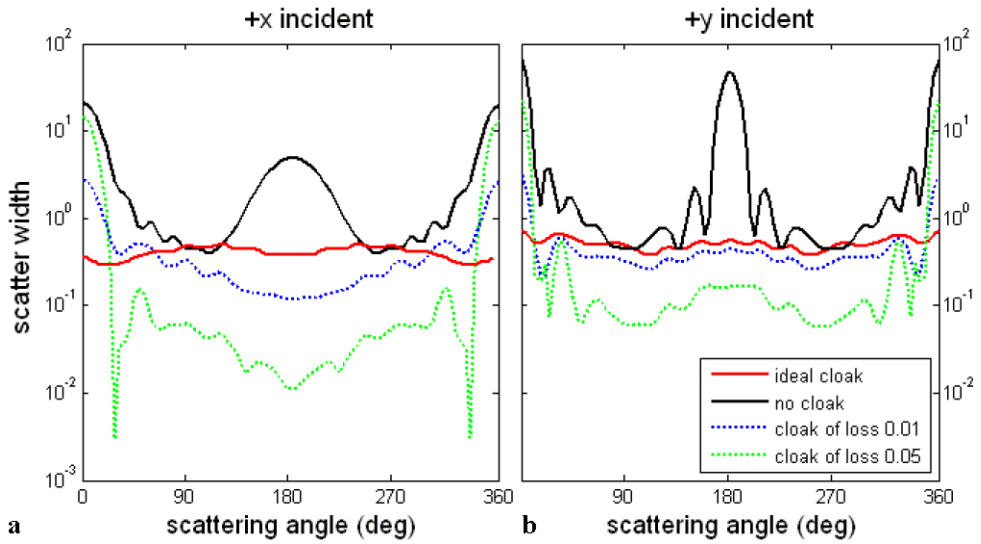

Fig. 6 The scattering width (normalized to the wavelength λ) of the dissimilar rectangular cloak of different models. (**a**) Illuminating toward $+x$-direction. (**b**) Illuminating toward $+y$-direction

ness while n increases. This is especially ideal for the rectangular cloak. In addition, the uniform thickness cannot be achieved when the geometry degenerates to a diamond, although the thickness of the cloak shell is still limited effectively.

2.3 Cloak for irregular regions

The design method proposed above is not just limited to the superellipses or dissimilar cloaks. Since the essential recipe of this approach involves (2) and (5), cloaks for irregular regions can be achieved if the analytic polar equations of the inner and outer boundaries are available. Moreover, the material parameters do not involve discontinuities as long as the boundaries are everywhere differentiable, i.e. do not possess sharp corners.

3 Results and discussion

In order to verify the behavior of the cloak devices in full-wave simulations, we compute several examples by using the COMSOL Multiphysics, which is based on the finite element method. In all the examples presented below, we keep $x_0 = 3$, $y_0 = 1$, $a = 0.15$ m, $b = 0.05$ m for the inner boundary, and $x_0 = 2$, $y_0 = 1$, $a = 0.20$ m, $b = 0.10$ m for the outer boundary for convenience of comparison. The incident field is set to be a 3 GHz TE polarized wave. The inner objects are chosen as perfect electric conducting (PEC) cylinders so that the fields inside are identically zero. Perfect matched layers (PML) are added around to terminate the computed region in coordinate directions.

Figures 2(a) and (b) show the simulating results of a dissimilar elliptic cloak device illuminated by a plane wave from left to right and a cylindrical wave from the lower left,

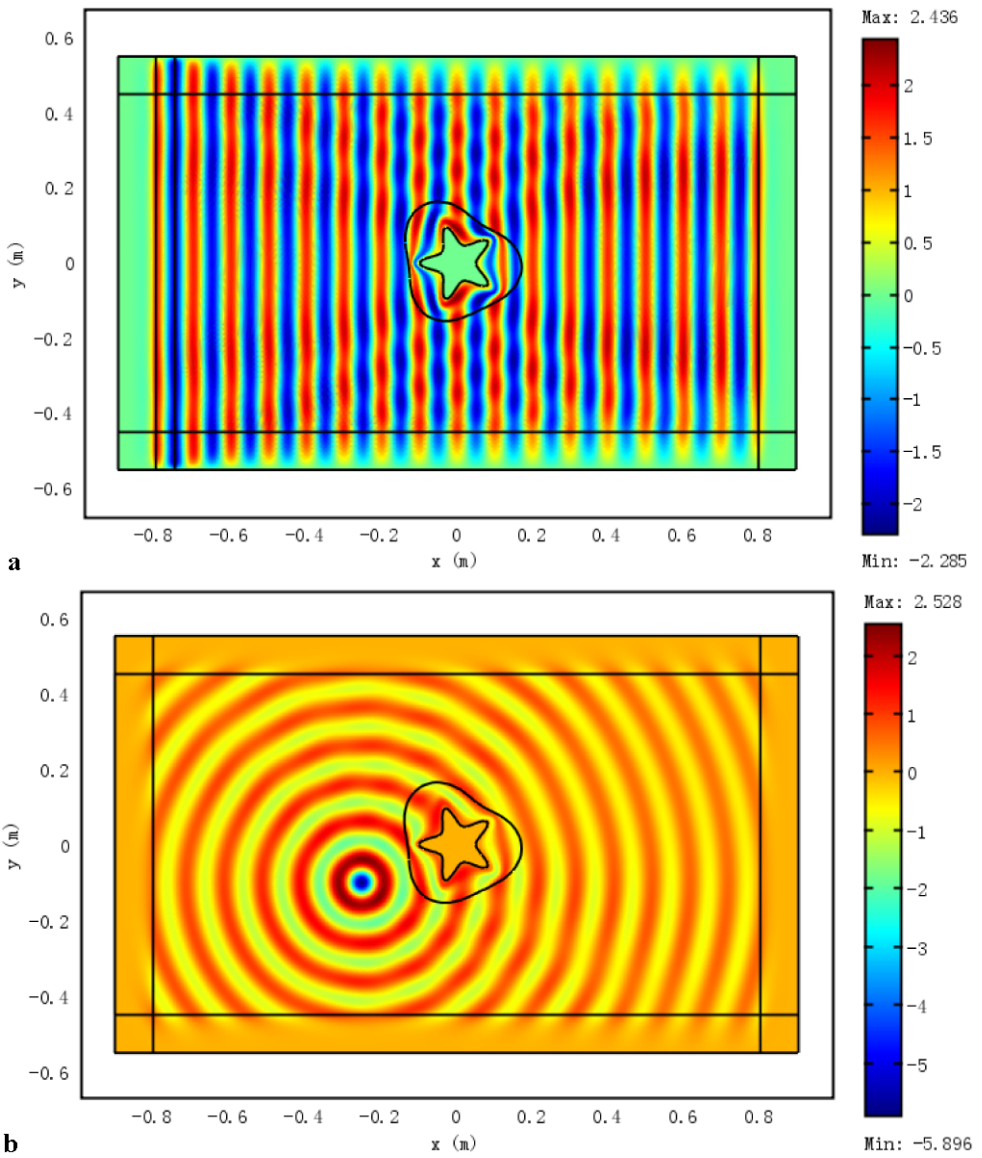

Fig. 7 Simulation results of the total electric-field distribution for an arbitrary dissimilar case

respectively. It is seen that fields through the cloaking shell are bent smoothly around the inner ellipses in both cases. Notice that the phase fronts at the left and right sides of the annular are compressed remarkably. The interpretation is straightforward, i.e. the device has to bend the trajectories and fields in smaller regions because the thickness in those directions is limited. Meanwhile, the field distributions outside the shell are almost unaltered. Figure 2(b) also gives a demonstration of the validity of the device when illuminated from different orientations.

Figures 3(a) and (b) illustrate the material parameters on the outer boundaries for the dissimilar cloak and similar cloak, respectively. Only the parameters for 0–180° are shown for symmetry. It can be seen that the parameters for the dissimilar cloak in Fig. 3(a) vary much faster than the ones for the similar cloak in Fig. 3(b), and the absolute values of the parameters in Fig. 3(a) are always larger. This is because the cloaking effect is carried out via a thinner shell in the former case. Another obvious difference between Figs. 3(a) and (b) is, noticing the blue lines, that the parameter ε_{zz} is no longer constant in Fig. 3(a). The phenomenon is caused by the nonlinear relation in (5). Since neither the determinant of the Jacobian matrix nor the factor r' is constant on the outer boundary, ε_{zz} varies with θ according to (2).

The illustrations for an approximate rectangular cloak are shown in Figs. 4(a) and (b), where we choose $n = 20$ for the superellipse. Although excluding the incident fields from the inner object is more difficult due to the existence of corners, the device displays a complete cloaking performance. Furthermore, the thickness for the annular is almost uniform, which shows the main advantage of this dissimilar cloak.

To investigate the material parameters of the rectangular cloak, we plot the tensors in two cases. Figure 5(a) shows the parameters for a dissimilar cloak. In contrast to the elliptic case in Fig. 4(a), we can recognize the effect of the corners, revealed by the two peaks for ε_{xx} (red line), and deep slopes for $\varepsilon_{xy}, \varepsilon_{yy}, \varepsilon_{zz}$. The same phenomena can be observed in Fig. 5(b), which represents the similar rigorous case. According to Fig. 5(b), parameter discontinuities exist at the sharp corners, bringing fabricating problems. However, the discontinuities are eliminated by the rounded approximation of the superellipse, despite choosing a large index $n = 20$. The cost is that ε_{zz} varies with θ at the corners, as mentioned in the elliptic case, and maintains constant with ε_{yy} on the straight sides.

In order to quantitatively evaluate the cloaking performance, the scattering width (the 2D equivalent of RCS) [18] is calculated for the dissimilar rectangular case. The scattering patterns of horizontal and vertical illuminating are shown in Figs. 6(a) and (b). In both cases, the forward (0°) and backward (180°) scatter is greatly reduced by comparing the red lines with the black lines, and the scattering width of the device with cloaks is smaller than that without cloaks for nearly all cases. The average ratios between the scattering widths with and without cloaks are over 8 and 10 for cases (a) and (b), respectively, and can be improved if a finer mesh is adopted in the calculation. Furthermore, loss tangents of 0.01 and 0.05 are added for realism considerations. The blue and green dotted lines in Fig. 6 reveal obvious scatter in the forward direction; on the other hand, the equivalent lengths in other directions are even smaller than in the ideal cloak. Considering the topological interpretation of transformation optics, this occurs because the lossy factor only operates as an absorber, while rays (which represent the power flow) in the cloak shell are almost unaltered [3]. As a result, the main forward- traveling power is strongly absorbed, impeding the field rebuilding in front, and the tiny scattered power flow in other directions is unavoidably absorbed, becoming even weaker.

Figure 7 gives an example for an arbitrary shape to show the universality of the method. As seen, the device performs well despite the complex, dissimilar boundaries.

4 Conclusion

A general method to design a 2D dissimilar cloak for irregular regions has been proposed by applying a nonlinear transformation in polar coordinates. The design avoided discontinuities in the material parameters while effectively limiting the thickness of the cloak shell. Full-wave simulations were performed and the scattering widths were calculated for different models to confirm the validity of the design. This method provides a possible access to cloak complex shaped objects.

Acknowledgements This work was supported by the National Natural Science Foundation of China (60501018), the National Basic Research Program of China under Grant (2004CB719800), and the Knowledge Innovation Program of the Chinese Academy of Sciences.

References

1. J.B. Pendry, D. Schurig, D.R. Smith, Science **312**, 1780 (2006)
2. D. Schurig, J.B. Pendry, D.R. Smith, Opt. Express **14**, 9794 (2006)
3. S.A. Cummer, B.-I. Popa, D. Schurig, D.R. Smith, J.B. Pendry, Phys. Rev. E **74**, 036621 (2006)
4. D. Schurig, J.J. Mock, B.J. Justics, S.A. Cummer, J.B. Pendry, A.F. Starr, D.R. Smith, Science **314**, 977 (2006)
5. W. Cai, U.K. Chettiar, A.V. Kildishev, V.M. Shavlaev, Nat. Photonics **1**, 224 (2007)
6. Y. Huang, Y. Feng, T. Jiang, Opt. Express **15**, 11133 (2007)
7. H. Chen, Z. Liang, P. Yao, X. Jiang, H. Ma, C.T. Chan, Phys. Rev. B **76**, 241104(R) (2007)
8. H. Chen, B.-I. Wu, B. Zhang, J.A. Kong, Phys. Rev. Lett. **99**, 063903 (2007)
9. H. Chen, C.T. Chan, Appl. Phys. Lett. **90**, 241105 (2007)
10. W. Yan, M. Yan, Z. Ruan, M. Qiu, New J. Phys. **10**, 043040 (2008)
11. S.A. Cummer, D. Schurig, New J. Phys. **9**, 45 (2007)
12. M. Rahm, D. Schurig, D.A. Roberts, S.A. Cummer, D.R. Smith, J.B. Pendry, Photonics Nanostruct. Fundam. Appl. **6**, 87 (2008)
13. D.-H. Kwon, D.H. Werner, Appl. Phys. Lett. **92**, 013505 (2008)
14. H. Ma, S. Qu, Z. Xu, J. Zhang, B. Chen, J. Wang, Phys. Rev. A **77**, 013825 (2008)
15. K. Yao, C. Li, F. Li, Chin. Phys. Lett. **25**, 1657 (2008)
16. W.X. Jiang, T.J. Cui, G.X. Xu, X.Q. Lin, Q. Cheng, J.Y. Chin, J. Phys. D **41**, 085504 (2008)
17. Y. You, G.W. Kattawat, P.W. Zhai, P. Yang, Opt. Express **16**, 6134 (2008)
18. C. Li, F. Li, Opt. Express **16**, 13414 (2008)
19. R. Weder, arXiv:0704.0248v4
20. R. Weder, J. Phys. A, Math. Theor. **41**, 065207 (2008) (21pp)
21. R. Weder, J. Phys. A, Math. Theor. **41**, 415401 (2008) (17pp)
22. D.-H. Kwon, D.H. Werner, Appl. Phys. Lett. **92**, 113502 (2008)
23. J. Hu, X. Zhou, G. Hu, arXiv:0808.3623
24. H. Chen, X. Zhang, X. Luo, H. Ma, C.T. Chan, New J. Phys. **10**, 113016 (2008)
25. E.J. Post, *Formal Structure of Electromagnetics* (Wiley, New York, 1962)